

Dielectric, conductivity and modulus analysis of AuGe/SiO₂/p-Si/AuGe capacitor

A. BÜYÜKBAŞ^a, A. TATAROĞLU^{a,*}, M. BALBAŞI^b

^aDepartment of Physics, Faculty of Science, Gazi University, Ankara, Turkey

^bDepartment of Chemical Engineering, Faculty of Engineering, Gazi University, Ankara, Turkey

In this study, the dielectric, conductivity and modulus properties of AuGe/SiO₂/p-Si/AuGe capacitor with interfacial thermal oxide layer were investigated using impedance measurements. These measurements were carried out in a wide frequency range. Dielectric parameters such as dielectric constant (ϵ'), loss (ϵ''), loss tangent ($\tan \delta$), ac conductivity (σ_{ac}), and real (M') and imaginary (M'') component of complex electric modulus (M^*) values were calculated from impedance measurements. Experimental results show that the values of dielectric parameters are a strong function of frequency.

(Received June 2, 2014; accepted June 24, 2015)

Keywords: MOS capacitor; Dielectric parameters; Ac conductivity; Modulus

1. Introduction

The metal-oxide-semiconductor (MOS) capacitor constitutes a kind of capacitor, which stores the electric charge by virtue of the dielectric property of oxide layer, and consists of a parallel-plate capacitor with one electrode a metallic plate, called the gate, and other electrode, the semiconductor. In other words, the basic MOS capacitor consists of an oxide film (such as SiO₂, SnO₂, TiO₂, Si₃N₄) sandwiched between a metal and semiconductor substrate. This oxide film can be grown by using different techniques such as thermal oxidation, chemical oxidation and rapid thermal oxidation [1-4]. A real MOS structure always contains defects so-called "charges" located in the bulk of the oxide or at the oxide-silicon interface. These charges are traditionally classified into four general types such as fixed oxide charge, mobile ionic charge, interface-trapped charge and oxide trapped charge [4,5]. Also, in MOS capacitor, three regions, which are the bulk oxide, the semiconductor/oxide interface and the oxide, in MOS capacitor are important in integrated circuit technology. Charges in all three regions play a role in integrated circuits [1,2].

In addition, the performance and stability of MOS capacitors depend on the formation and thickness of interfacial oxide layer, oxide leakage, interface trap densities and series resistance bulk doping profile [6-12].

Impedance spectroscopy (IS) is a powerful and widely used technique which is utilized to characterize the electrical properties of materials. It may be used to investigate the dynamics of bound or mobile charge in the bulk or interfacial regions of any kind of solid or liquid material: ionic, semiconducting, mixed electronic-ionic and even insulators (dielectrics) [13]. Also, this IS method has been used to characterize a wide range of materials. The IS is particularly characterized by the measurement and analysis of some or all of the four impedance-related

functions impedance (Z), admittance (Y), electric modulus (M), and dielectric permittivity (ϵ). Furthermore, from an impedance spectrum, both the structure of its equivalent circuit and the parameter values can be extracted [13-16].

The aim of the present paper is to investigate the effect of frequency on dielectric parameters of AuGe/SiO₂/p-Si/AuGe (MOS) capacitor. The frequency dependence of dielectric parameters such as dielectric constant (ϵ'), loss (ϵ''), loss tangent ($\tan \delta$), ac conductivity (σ_{ac}) and electric modulus obtained from impedance measurements were discussed in detail.

2. Experimental details

The thermal oxide wafer was purchased from MTI Corporation. The wafer, boron doped (p-type) single crystal Si substrate, has a 2" diameter, (100) orientation, and $<0.005 \Omega \cdot \text{cm}$ resistivity. Thermal oxide or silicon dioxide (SiO₂) layer with a thickness of 300 nm (3000 Å) is formed on bare silicon surface at 1000 °C, using a dry growth method. To form the ohmic and rectifier contacts of MOS capacitors were used a thermal evaporation system. First, the ohmic back contacts with a thickness of ~150 nm were formed by the deposition of AuGe (88:12 wt %) onto the whole back surface of the Si wafer at 400 °C and under 10^{-6} mbar vacuum. Then, the thermal oxide silicon wafer was annealed at 350 °C for 3 min to achieve good ohmic contact behaviour. Finally, rectifier front contacts with 2 mm diameter and ~120 nm thickness were formed by the deposition of AuGe onto the oxidized surface of the Si wafer under 10^{-6} mbar vacuum. Thus, AuGe/SiO₂/p-Si/AuGe (MOS) capacitor was fabricated for the electrical measurements. The electrode connections were made by silver paste.

The impedance measurements of the fabricated MOS capacitor were performed using a Solartron SI1260

Impedance/Gain-Phase analyzer. Besides, to obtain higher sensitivity in the high dielectric range, a Solartron 1296 Dielectric Interface was coupled to the analyzer. The impedance measurements as a function of the applied dc bias voltage were carried out in the frequency range of 100 Hz-1 MHz at room temperature. Also, a small ac test signal 100 mV_{rms} from the external pulse generator was applied to the capacitor in order to meet the requirements.

3. Results and discussion

The impedance spectroscopy is an experimental technique used for the electrical and dielectric properties of many electronic devices. Also, impedance spectroscopy was used to measure the response of the material to a small amplitude excitation over a wide frequency range. The MOS capacitor can be modeled by an equivalent electrical circuit shown in Fig. 1.

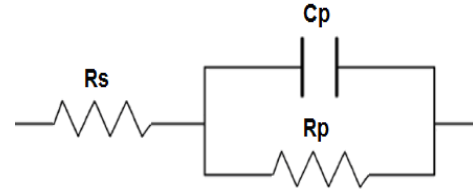


Fig. 1. Equivalent-circuit model in terms of a single parallel resistance R_p and capacitance C_p network with a series resistance R_s .

The equivalent electrical circuit consists of a single parallel resistance (bulk resistance, R_p) and capacitance (bulk capacitance, C_p) network with a series resistance (contact resistance, R_s). Therefore, the expression for the complex impedance of the equivalent circuit is giving by [13,17-21]

$$Z^*(\omega) = R_s + \frac{R_p}{1 + i\omega R_p C_p} = \left[R_s + \frac{R_p}{1 + (\omega R_p C_p)^2} \right] - i \left[\frac{\omega R_p^2 C_p}{1 + (\omega R_p C_p)^2} \right] = Z'(\omega) - iZ''(\omega) \quad (1)$$

Where Z' and Z'' are the real part and imaginary parts of the complex impedance, and ω is the angular frequency of the ac signal, $\omega = 2\pi f$.

The frequency dependent the real (Z') and imaginary part (Z'') of the complex impedance (Z^*) is shown in Fig. 2. As seen in Fig. 2, the values of the Z' decrease with the increasing frequency and remain constant at sufficiently high frequency ($f > 500$ kHz) [17-19,22-24]. The observed

decrement in the Z' with the increasing frequency confirms the presence of interface states. The values of the Z'' initially increase with the increasing frequency, then reaches a maximum peak and finally decreases with further increases in frequency. Furthermore, the Z'' curve gives a peak and the peak shows the single relaxation process in the device.

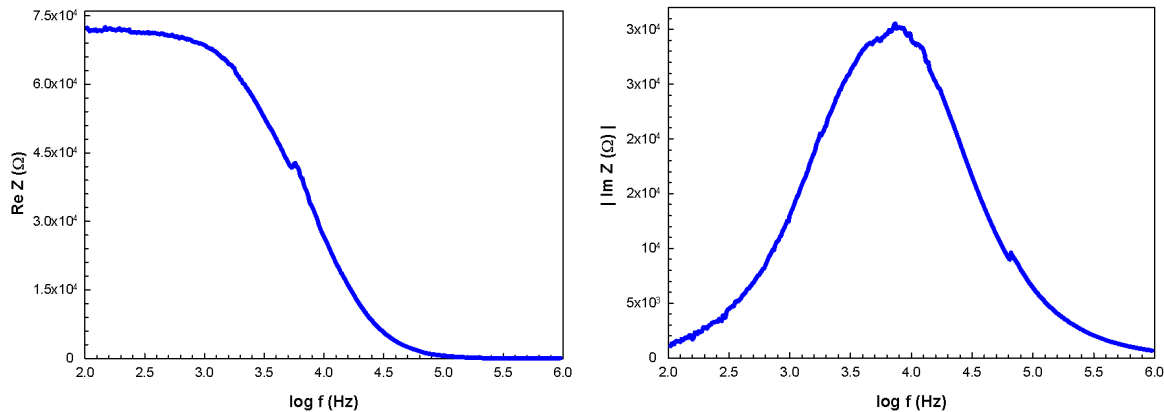


Fig. 2. The frequency dependent (a) real (Z') and (b) imaginary (Z'') part of the complex impedance.

Dielectric spectroscopy sometimes called as impedance spectroscopy is a method used to determine the dielectric characteristics of nonconducting or semiconducting materials in relation to their structure and also of electronic or sensor devices. Dielectric spectroscopy measures the dielectric permittivity as a function of frequency and temperature. Also, this method is based on the interaction of an external field with the electric dipole moment of the structure. The dielectric permittivity (ϵ^*) is expressed in the complex form: [25-28]

$$\epsilon^*(\omega) = \epsilon'(\omega) - i\epsilon''(\omega) \quad (2)$$

Where ϵ' and ϵ'' are the real and the imaginary parts of complex dielectric permittivity (ϵ^*), and $i = \sqrt{-1}$ the imaginary factor. In the case of impedance measurements, the Eq. (2) can be written as

$$\epsilon^* = \frac{1}{i\omega C_0 Z^*} = \frac{Z''}{\omega C_0(Z'^2 + Z''^2)} - i \frac{Z'}{\omega C_0(Z'^2 + Z''^2)} \quad (3)$$

Where C_0 ($=92.63$ pF) is capacitance of an empty capacitor and expressed as $C_0 = \epsilon_0 A / d_{ox}$, with A ($=3.14 \times 10^{-2}$ cm²) being the rectifier contact area in cm², d_{ox} ($=3000$ Å) the interfacial oxide layer thickness, and ϵ_0 the permittivity of free space charge ($\epsilon_0 = 8.85 \times 10^{-14}$ F/cm).

Dielectric loss tangent ($\tan\delta$) or dissipation factor, which means the phase difference due to the loss of energy within the structure, can be expressed as follows,

$$\tan\delta = \frac{Z''(\omega)}{Z'(\omega)} \quad (4)$$

The ac electrical conductivity (σ_{ac}) can be represented by the following equation,

$$\sigma_{ac} = \frac{d_{ox}}{AZ'(\omega)} = \epsilon_0 \omega \epsilon''(\omega) \quad (5)$$

The electric modulus approach began when the reciprocal complex permittivity was discussed as an electrical analogue to the mechanical shear modulus [29]. From the physical point of view, the electrical modulus corresponds to the relaxation of the electric field in the material when the electric displacement remains constant. Therefore, the modulus represents the real dielectric relaxation process. The complex electric modulus $M^*(\omega)$ was introduced to describe the dielectric response of non-conducting material. Also, this formalism has been applied to materials with non-zero conductivities. The electric modulus is expressed in the complex modulus formalism: [30-36]

$$M^*(\omega) = \frac{1}{\epsilon^*(\omega)} = i\omega C_0 Z^*(\omega) = M'(\omega) + iM''(\omega) \quad (6)$$

$$M'(\omega) = \frac{\epsilon'(\omega)}{\epsilon'(\omega)^2 + \epsilon''(\omega)^2} = \omega C_0 Z''(\omega) \quad \text{and}$$

$$M''(\omega) = \frac{\epsilon''(\omega)}{\epsilon'(\omega)^2 + \epsilon''(\omega)^2} = \omega C_0 Z'(\omega) \quad (7)$$

Where M' and M'' are the real and the imaginary parts of complex modulus.

The frequency dependences of the ϵ' , ϵ'' , $\tan\delta$, σ_{ac} , M' and M'' of the MOS capacitor obtained from admittance measurements at room temperature. The variations of dielectric parameters are shown in Figs. 3(a)-3(c), respectively. As seen in Fig. 3(a) and (b), the values of the dielectric constant (ϵ') and loss (ϵ'') decrease with the increasing frequency and remain almost constant at high

frequencies. This is the normal behavior of a dielectric material. The decreases in ϵ' and ϵ'' with the increasing frequency are explained by the fact that as the frequency is raised, the interfacial dipoles have less time to orient themselves in the direction of the alternating field [37-43].

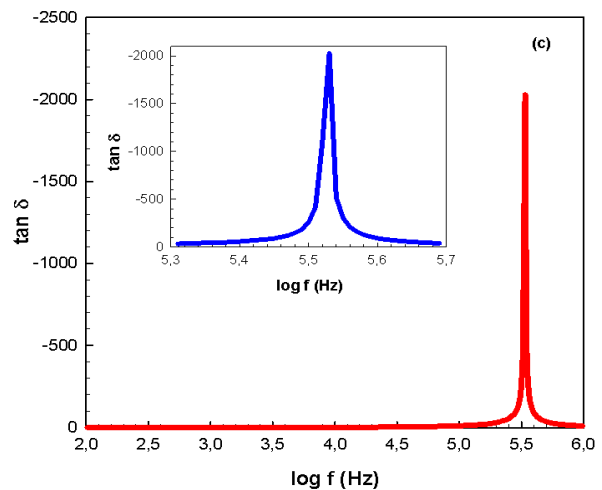
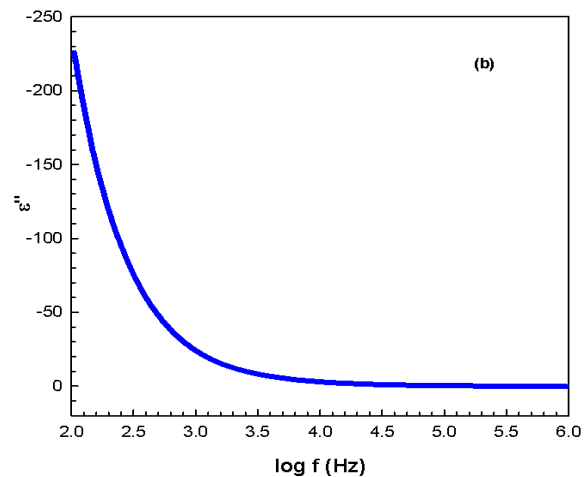
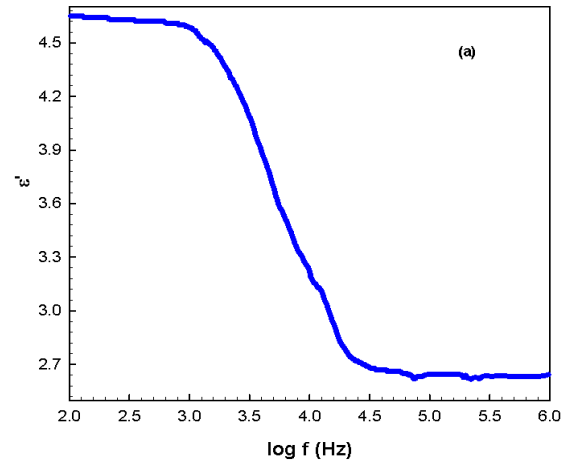


Fig. 3. Variations of the ϵ' (a), ϵ'' (b), and $\tan\delta$ (c) as a function of frequency.

As seen in Fig. 3(c), the value of dielectric loss tangent ($\tan\delta$) remains almost constant up to about 500 kHz. Then, the plot of $\tan\delta$ gives a peak. This peak suggests the presence of dielectric relaxation in the structure. In general, the dielectric relaxation process is determined by rate of polarization formed and frequency of applied electric field. Also, dielectric loss tangent is associated with the electrical conductivity.

Fig. 4 shows the variation of the ac electrical conductivity (σ_{ac}) with frequency. As seen in Fig. 4, the σ_{ac} increases slowly up to about 100 kHz but it decreases up to 500 kHz, and then it increases rapidly again with the increasing frequency. The frequency dependence of conductivity can be attributed to the relaxation phenomena arising from mobile charge carriers [44,45]. Also, the increase of σ_{ac} with increase in frequency also suggests the hopping conduction and the increase of the applied frequency enhances the hopping of charge carriers between the localized states [46-48].

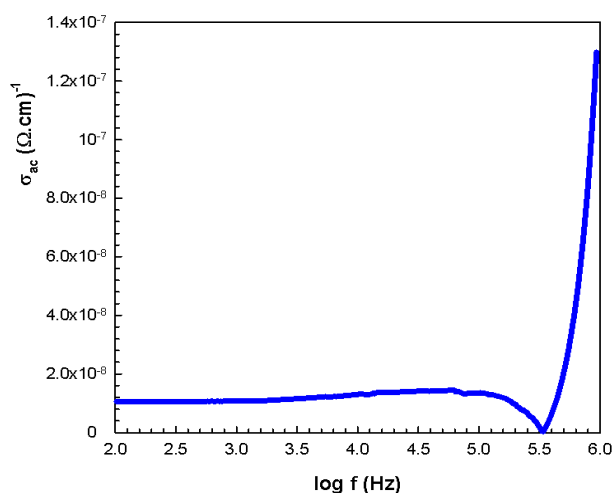


Fig. 4. Variation of ac electrical conductivity with frequency.

The variation real (M') and imaginary (M'') parts of the complex electrical modulus with frequency is given in Fig. 5(a) and (b). As seen in Fig. 5(a), the value of M' increases with the increasing frequency and remains almost constant at high frequencies. The increase of M' may possibly be related to a lack of restoring force governing the mobility of charge carriers under the action of an induced electric field. As seen in Fig. 5(b), the M'' increases with the increasing frequency but it gives a peak at about 10 kHz, and then it decreases with the increasing frequency. The region where the peak occurs is indicative of the transition from long-range to short-range mobility with increase in frequency [30,32,33,49-53]. Also, this observed peak is a relaxation peak. Relaxation time for the relaxation process was determined from the relaxation curves. The relaxation time (τ) has been calculated using the relation $\tau \times 2\pi f_{max} = 1$, where f_{max} is the peak frequency. The value of f_{max} and τ is found to be about 10^4 Hz and 1.59×10^{-5} s, respectively.

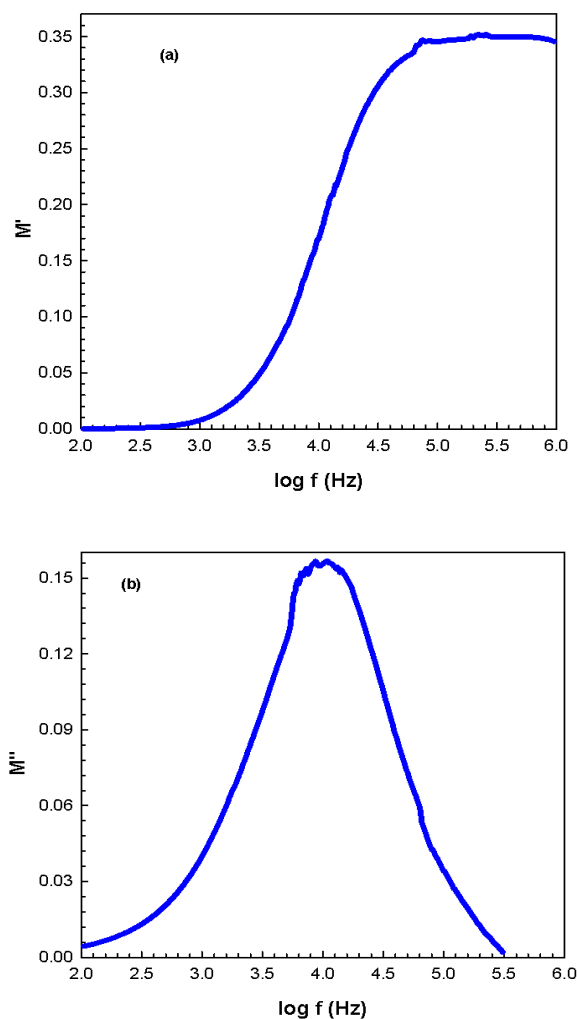


Fig. 5. Variation of (a) real (M') and (b) imaginary (M'') parts of complex modulus with frequency.

4. Conclusion

The dielectric, conductivity and modulus properties of AuGe/SiO₂/p-Si/AuGe capacitor have been investigated by using impedance measurements. The frequency dependent real (Z') and imaginary (Z'') parts of complex impedance were fitted using equivalent circuit. The values of the dielectric constant (ϵ'), loss (ϵ''), loss tangent ($\tan\delta$), ac conductivity (σ_{ac}), and real (M') and imaginary (M'') component of complex electric modulus (M^*) values were obtained from impedance measurements. The decreases in ϵ' and ϵ'' with increase in frequency are explained by the fact that as the frequency is raised, the interfacial dipoles have less time to orient themselves in the direction of the alternating field. The ac electrical conductivity (σ_{ac}) increase with the increasing frequency due to the accumulation of charge carries at the boundaries. Also, the plot of M'' gives a relaxation peak. The relaxation time (τ) has been calculated from the peak frequency.

References

- [1] E.H. Nicollian, J.R. Brews, MOS Physics and Technology, Wiley, New York, 1982.
- [2] S.M. Sze, Physics of Semiconductor Devices, 2nd Ed., Wiley, New York, 1981.
- [3] A.S. Grove, Physics and Technology of Semiconductor Devices, Wiley, New York, 1967.
- [4] H. Bentarzi, Transport in Metal-Oxide-Semiconductor Structures, Springer, New York, 2011.
- [5] B.E. Deal, IEEE Trans. Elect. Dev. ED-27, 606 (1980).
- [6] A. Tataroğlu, Ş. Altındal, Vacuum, **82**, 1203 (2008).
- [7] Ş. Kaya, R. Lok, A. Aktağ, J. Seidel, E. Yılmaz, J. Alloys Compd. **583**, 476 (2014).
- [8] Ş. Karataş, F. Yakuphanoğlu, F. M. Amanullah, J. Phys. Chem. Solids **73**, 46 (2012).
- [9] J. Panda, S. Chattopadhyay, T.K. Nath, J. Appl. Phys. **114**, 224508 (2013).
- [10] A. Tataroğlu, Ş. Altındal, Microelectron. Eng. **85**, 2256 (2008).
- [11] H. M. Baran, A. Tataroğlu, Chin. Phys. B **22**, 047303 (2013).
- [12] M. Sharma, S.K. Tripathi, Appl. Phys. A **113**, 491 (2013).
- [13] E. Barsoukov, J.R. Macdonald, Impedance Spectroscopy Theory, Experiment, and Applications, 2nd Ed., Wiley, New Jersey, 2005.
- [14] O. Kanoun, Lecture Notes on Impedance Spectroscopy: Measurement, Modeling and Applications, Taylor, London, 2011.
- [15] R.A. Gerhardt, "Impedance Spectroscopy and Mobility Spectra," Chapter in Encyclopedia of Condensed Matter Physics, Elsevier Press, 350-363, 2005.
- [16] V.F. Lvovich, Impedance Spectroscopy: Applications to Electrochemical and Dielectric Phenomena, Wiley, New Jersey, 2012.
- [17] S.H. Kim, S.C. Lim, J.H. Lee, T. Zyung, Curr. Appl. Phys. **5**, 35 (2005).
- [18] Y. Liu, A. Liu, Z. Hu, W. Liu, F. Qiao, J. Phys. Chem. Solids **73**, 626 (2012).
- [19] L. Bi-Xin, C. Jiang-Shan, Z. Yong-Biao, M. Dong-Ge, Chin. Phys. Lett. **28**, 057201 (2011).
- [20] P.P. Sahay, R.K. Mishra, S.N. Pandey, S. Jha, M. Shamsuddin, Ceramics Inter. **38**, 1281 (2012).
- [21] A. Büyükbaş, A. Tataroğlu, M. Balbaşı, J. Nanoelectron. Optoelectron. **9**, 515 (2014).
- [22] G. Chauhan, R. Srivastava, P. Tyagi, A. Kumar, P.C. Srivastava, M.N. Kamalasanan, Synth. Met. **160**, 1422 (2010).
- [23] M.M. Costa, G.F.M. Pires Júnior, A.S.B. Sombra, Mater. Chem. Phys. **123**, 35 (2010).
- [24] C.K. Suman, J. Yun, S. Kim, S.D. Lee, C. Lee, Curr. Appl. Phys. **9**, 978 (2009).
- [25] A. Chelkowski, Dielectric Physics, Elsevier, Amsterdam, 1980.
- [26] M. Popescu, I. Bunget, Physics of Solid Dielectrics, Elsevier, Amsterdam, 1984.
- [27] C.P. Symth, Dielectric Behaviour and Structure, McGraw-Hill, New York, 1955.
- [28] V.V. Daniel, Dielectric Relaxation, Academic Press, London, 1967.
- [29] N.G. McCrum, B.E. Read, G. Williams, Anelastic and Dielectric Effects in Polymeric Solids, Wiley, New York, 1967.
- [30] M. Ram, S. Chakrabarti, J. Phys. Chem. Solids **69**, 905 (2008).
- [31] S.V. Rathan, G. Govindaraj, Solid State Ionics **181**, 504 (2010).
- [32] A. Tataroğlu, G.U. J. Sci. **26**, 501 (2013).
- [33] K.P. Padmasree, D.K. Kanchan, Mater. Sci. Eng. B **122**, 24 (2005).
- [34] F. Yakuphanoğlu, I.S. Yahia, B.F. Senkald, G.B. Sakrc, W.A. Farooq, Synthetic Metals **161**, 817 (2011).
- [35] T. Ataseven, A. Tataroğlu, Chin. Phys. B **22**, 117310 (2013).
- [36] İ. Dökme, Ş. Altındal, T. Tunç, İ. Uslu, Microelectron. Reliab. **50**, 39 (2010).
- [37] S. Maity, D. Bhattacharya, S.K. Ray, J. Phys. D: Appl. Phys. **44**, 095403 (2011).
- [38] Md M. Hoque, A. Dutta, S. Kumar, T.P. Sinha, Physica B **407**, 3740 (2012).
- [39] D.E. Yıldız, D.H. Apaydın, L. Toppare, A. Cırpan, J. Appl. Polym. Sci. **128**, 1659 (2013).
- [40] A. Tataroğlu, İ. Yücedağ, Ş. Altındal, Microelectron. Eng. **85**, 1518 (2008).
- [41] S.P. Szu, C.Y. Lin, Mater. Chem. Phys. **82**, 295 (2003).
- [42] H.M. Chenari, M.M. Golzan, H. Sedghi, A. Hassanzadeh, M. Talebian, Curr. Appl. Phys. **11**, 1071 (2011).
- [43] T. Ataseven, A. Tataroğlu, T. Memmedli, S. Özçelik, J. Optoelectron. Adv. Mater. **14**(7-8), 640 (2012).
- [44] A.K. Jonscher, Nature, **267**, 673 (1977).
- [45] A. Chaouchi, S. Kennour, Process. Appl. Ceramics **6**, 201 (2012).
- [46] Y.A. El-Gendy, I.S. Yahia, F. Yakuphanoglu, Mater. Res. Bulletin **47**, 3397 (2012).
- [47] S. Dutta, R.N.P. Choudhary, P.K. Sinha, Ceram. Int. **33**, 13 (2007).
- [48] A. Tataroğlu, J. Optoelectron. Adv. Mater. **13**, 940 (2011).
- [49] F. Yakuphanoglu, D.D. Zaitsev, L.A. Trusov, P.E. Kazin, J. Magn. Mater. **312**, 43 (2007).
- [50] R. Ertuğrul, A. Tataroğlu, Chin. Phys. Lett. **29**(7), 077304 (2012).
- [51] M.B. Mohamed, H. Wang, H. Fuess, J. Phys. D: Appl. Phys. **43**, 455409 (2010).
- [52] M. Ram, S. Chakrabarti, J. Alloys Compd. **462**, 214 (2008).
- [53] A.K. Jonscher, Universal Relaxation Law, Chelsea Dielectric Press, London, 1996.

*Corresponding author: ademt@gazi.edu.tr